Modeling of current-voltage characteristics in large metal - semiconducting carbon nanotube systems

Toshishige Yamada[a)]

NASA Ames Research Center, M/S T27A-1, Moffett Field, California, 94035-1000

A model is proposed for two observed current-voltage (I-V) patterns in recent experiment with a scanning tunneling microscope tip and a carbon nanotube [Collins et al., Science **278**, 100 (1997)]. We claim that there are two contact modes for a tip (metal)-nanotube (semiconductor) junction depending whether the alignment of the metal and the semiconductor band structures is (1) variable (vacuum-gap) or (2) fixed (touching) with V. With the tip grounded, the tunneling case in (1) would produce large dI/dV with $V > 0$, small dI/dV with $V < 0$, and $I = 0$ near $V = 0$ for an either n- or p-nanotube. However, the Schottky mechanism in (2) would result in forward current with $V < 0$ for an n-nanotube, while with $V > 0$ for an p-nanotube. The two observed I-V patterns are thus entirely explained by a tip-nanotube contact of the two types, where the nanotube must be n-type. We apply this model to the source-drain I-V characteristics in a long nanotube-channel field-effect-transistor with metallic electrodes at low temperature [Zhou et al., Appl. Phys. Lett. **76**, 1597 (2000)], and show that two independent metal-semiconductor junctions in series are responsible for the observed behavior.

Introduction

Recently, current-voltage (I-V) characteristics have been reported for a system with a scanning tunneling microscope (STM) tip and a carbon nanotube at room temperature [1]. The STM tip was driven forward into a film of many entangled nanotubes on a substrate, and then was retracted well beyond the normal tunneling range. At a distance of ~ 0.1 μm above the surface, there was usually an electronic conduction between the tip and the film since nanotubes bridged the two regions. At ~ 1 μm, only one nanotube remained occasionally, and the electronic conduction was still maintained. One end of the nanotube continued sticking to the tip during the retraction, while the other remained in the film. I-V characteristics for this tip-nanotube system had two different patterns for low (< 1.95 μm) and high (1.98 μm) tip-to-film distances. The lower-distance cases showed large dI/dV with $V > 0$, small dI/dV with $V < 0$, and $I = 0$ near $V = 0$ (type-I) as shown in Fig. 1(a), while the high-distance case showed rectification, i.e., $I \neq 0$ only with $V < 0$ (type-II) as in Fig. 1(b), if the tip was grounded (opposite bias definition from [1]). Although the experiment was performed in the early days of nanotube research, this is one of the rare reports confirming two I-V patterns in essentially the same experimental setup, both of which are expected for metal-semiconductor junctions.

We consider that the observed characteristics strongly reflected the nature of the tip (metal) - nanotube (semiconductor) contact. The other end of the nanotube was entangled well in the film, and simply provided a good Ohmic contact. We will argue that there are two different contact modes - vacuum gap (left) and touching (right) modes as schematically shown in Fig. 1(c), depending on whether the alignment of the metal and the semiconductor band structures is variable (vacuum-gap) or fixed (touching) with V. These modes would be related to physisorption and chemisorption, respectively. The "vacuum-gap" here means the absence of a conducting material

in the gap, and even if there exists a dielectric material, this mode can be used with a re-evaluation of the dielectric constant. Once admitting their existence, it is naturally shown that *I-V* characteristics are type-I in the vacuum-gap mode, and type-II in the touching mode. We will show that the nanotubes were *n*-type when hanging in air, contrary to the *p*-type behavior when placed on the silicon-dioxide layer in the field-effect-transistor (FET) applications [2].

The present model can be widely applied to other cases whenever a semiconducting nanotube is contacted by a large metal. As an example, we will explain the source-drain *I-V* characteristics of a long-nanotube channel FET with metallic electrodes at low temperature [3] as a signature of two metal-semiconductor junctions in the vacuum-gap mode that are back-to-back connected in the source-channel-drain structure.

Mechanisms for two I-V patterns in STM tip-nanotube system

In experiment [1], the STM tip was not placed at the end of the nanotube as if it were an extension sharing the same cylinder axis, but contacted the side of the nanotube so that the tip and nanotube surfaces faced each other. Thus, one-dimensional cylinder junction effects, such as the exponential dependence of depletion layer width on the inverse doping, or the long tail of the charge distribution [4], are not relevant here. Additionally, nanotubes will generally flatten on a substrate due to the van der Waals interaction [5]. Thus, a nanotube will flatten at the STM tip surface in both contact modes shown in Figs. 1(c) and 1(d). Therefore, the tip-nanotube junction is even better approximated by the traditional planar junction model [6], and then the familiar energy band diagrams prevail.

We study the electronic properties with band diagrams first for *n*-nanotubes and then for *p*-nanotubes, respectively. Figure 2 refers to the *n*-nanotube case: (a) is a type-I *I-V* pattern and (b) -

(d) are corresponding band diagrams in the vacuum-gap mode; (e) is a type-II *I-V* pattern and (f) - (h) are corresponding band diagrams in the touching mode. In the STM tip (metal) side, E_{FM} is the Fermi energy and ϕ_M is the work function. In the *n*-nanotube (semiconductor) side, χ is the electron affinity, E_{FS} is the Fermi energy (electrochemical potential), and E_G is the band gap. E_c and E_v are conduction and valence band edges, respectively, and depend on the applied voltage V after the tip is grounded. ϕ_n and ϕ_p are Schottky barriers for electrons and holes, respectively, and $\xi = E_{FS} - E_v$ is a chemical potential. At (b), valence-band electrons tunnel to the tip with $V < 0$, resulting in smaller *dI/dV* because of the higher vacuum barrier. (c) is a thermal equilibrium with $V = 0$. At (d), electrons on the tip tunnel to the conduction band with $V > 0$, resulting in larger *dI/dV* because of the lower vacuum barrier. Therefore, the role of the vacuum gap is to provide freedom for the system to adjust E_c and E_v with respect to the grounded metal Fermi energy E_{FM} by allowing a necessary voltage drop there. In the touching mode, ϕ_n and ϕ_p are fixed regardless of V and this provides a mechanism for rectification. These two modes result in fundamentally different *I-V* characteristics, type-I and type-II, respectively. In the experiment [1], $I \neq 0$ in the touching mode was associated with the smaller *dI/dV* in the vacuum-gap mode. This statement is valid regardless of the bias polarity definition. We interpret that the Schottky forward transport occurred at the same bias polarity as the *valence*-band tunneling of (b). Since band diagram (f) follows with the same polarity as (b), i.e., $V < 0$, the Schottky barrier is ϕ_n and the nanotube must be *n*-type. (g) is a thermal equilibrium. (h) is a reverse condition resulting in $I = 0$ with $V > 0$.

The *I-V* characteristics are *qualitatively* different for *p*-nanotubes as shown in Fig. 3. The entire *I-V* pattern in the vacuum-gap mode simply shifts to the positive V direction as in (a), reflecting the difference in ξ as shown in the band diagrams (b) - (d). The valence-band tunneling still occurs with $V < 0$, and the conduction band tunneling occurs with $V > 0$. However, the *I-V*

pattern in the touching mode is π-rotated around the origin as in (e), and this is because ϕ_p is now a Schottky barrier and the forward/backward transport occurs at the opposite bias polarity as in the band diagrams (f) - (h). Therefore, the Schottky forward transport occurs at the same bias polarity as the *conduction*-band tunneling, or $I \neq 0$ in the touching mode is associated with the *larger dI/dV* in the vacuum-gap mode. This is contrary to the experimental results [1], providing a solid foundation for claim that the nanotube was *n*-type.

In the FET experiment [2,3,7], a semiconducting channel nanotube was contacted by metallic source and drain electrodes. The nanotubes were found consistently *p*-type on the silicon-dioxide layer regardless of their channel length, based on the observation that the increasing channel conductance with swinging the gate voltage in the large negative direction. However, it has to be emphasized that the measurement detected the carrier concentration rather than the impurity concentration. Then it is not surprising that the nanotubes hanging in air were *n*-type while the nanotubes placed on the silicon-dioxide layer were *p*-type. In fact, this is similar to what we experienced for metal-oxide-semiconductor (MOS) transistors a few decades ago [6,8]. Nanotubes are *n*-type when they are produced, due to the unintentional, systematic inclusion of particular impurity atoms. Thus, nanotubes are *n*-type in air. Now, silicon-dioxide layers are known to include infamous trapped charges [6,8]. In an FET structure, the opposite charges are attracted by these trapped charges in the silicon-dioxide layer, and flow out of the source and the drain electrodes (charge reservoirs) to the nanotube channel. These incoming opposite charges can raise or lower the Fermi energy significantly *without changing* the initial impurity concentration. Thus, the nanotubes attached to electrodes on the silicon-dioxide layer can behave as *p*-type, regardless of the initial impurity concentration. Historically, a large change in the threshold voltage of a MOS transistor (the Fermi energy in the silicon channel) had been a mystery, but it was finally

found that the trapped charges in the silicon-dioxide layer were responsible due to the above mechanism [6,8]. In the context of nanotube research, the impurities causing the *n*-type in air and the trapped charges causing the *p*-type on the silicon-dioxide have not been identified yet.

Formulation for vacuum-gap and touching modes

For the touching mode, the familiar Schottky equation [6] should prevail and we use it extensively in the present analysis. For the vacuum-gap mode, we need a little preparation. We assume that the total energy E and the momentum $k_\rho = (k_x^2 + k_y^2)^{1/2}$ parallel to the STM tip-nanotube interface are conserved in the tunneling [9], where k_x and k_y are transverse and longitudinal momenta of an electron in the nanotube, respectively. Generally, momentum is conserved when the contact is infinitely large in that direction [10]. Thus, k_y is conserved since nanotubes are usually long enough. The nanotube used in the experiment is considered to be sufficiently wide (allowing many subbands) that we can assume the k_ρ-conservation. In this wide limit, subbands can be treated with a continuum model. We perform a k_ρ-integration with the effective mass m_i for band i ($i = c, v$) instead of a summation over the relevant modes. At absolute zero temperature, the tunneling current I_i between the metallic STM tip and the band i of the semiconducting nanotube through the vacuum barrier is given [9,11] by,

$$I_i = \frac{eS}{2\pi h}\int_{E_{FM}-eV}^{E_{FM}} dE\,\theta[\pm(E-E_i)]\int dk_\rho^2 D(E,k_\rho^2) \quad , \qquad (1)$$

where e is the unit charge, h the Planck constant, and S is an overlap area between the tip and the nanotube. θ is a step function, and E_i's are nanotube band edges. The + sign is for I_c with E_c, and - sign is for I_v with E_v. The tip (E_{FM}) is grounded, so that E_{FS} is equal to E_{FM} - eV. The band edges are given by $E_v(V) = E_{FM}$ - eV - ξ and $E_c(V) = E_v(V) + E_G$, respectively, where the chemical

potential ξ is V-independent. $D(E, k_\rho^2)$ is a transmission coefficient of an electron through the vacuum barrier with width d. These quantities are schematically shown in the band diagrams in Figs. 2 and 3.

We define $W = E - \gamma k_\rho^2$, the z-component (perpendicular to the STM tip-nanotube interface) energy in the metal with $\gamma = h^2/8\pi^2 m$, where m is the vacuum electron mass. Assuming that $D(E, k_\rho^2)$ depends only on W [11], we change the integration variable from k_ρ^2 to W. Due to the parallel momentum - energy conservation, we have $E = \pm\gamma(k_\rho^2 + k_{zS}^2)/\alpha_i + E_i = \gamma(k_\rho^2 + k_{zM}^2)$, where k_{zS} and k_{zM} are z-component momenta in the semiconductor and in the metal, respectively, and α_i is the effective mass m_i for band i normalized to m. The + sign is for $i = c$, and the - sign is for $i = v$. We note that $\delta = \pm\alpha_i(E - E_i) > 0$ for both cases. The range of W-integration is not from 0 to E because of this relation. This situation is best visualized by plotting γk_{zS}^2 and γk_{zM}^2 (= W) as functions of γk_ρ^2 with E and δ as parameters in Fig. 4. Both γk_{zS}^2 and γk_{zM}^2 must stay positive. This defines the domain $0 \le \gamma k_\rho^2 \le \delta$ as shown with a thick segment on the x-axis. This is converted to the range for W, the thick segment on the y-axis. Thus, $E - \delta = E \pm \alpha_i(E_i - E) \le W \le E$.

We consider a *semiconducting* (17,0) nanotube with a diameter of 1.33 nm, which is the closest to the experimental estimation at 1.36 nm [1] in the zigzag tube families [12]. All the band related values are calculated based on the tight-binding method [12]. We evaluate m_i by averaging the inverse masses for 17 subbands, and find $\alpha_c = \alpha_v = 0.216$. Changing the integration variable to W, we have [9,11],

$$I_i = \frac{4\pi meS}{h^3}\int_{E_{FM}-eV}^{E_{FM}} dE\,\theta[\pm\{E - E_i(V)\}]\int_{E \pm \alpha_i(E_i(V)-E)}^{E} dW D(W) \quad , \quad (2)$$

where $E_G = 0.54$ eV for the (17,0) nanotube [12]. In forming a nanotube from a graphite sheet, a band gap opens symmetrically from the graphite Fermi energy according to the tight-binding pic-

ture [12]. Thus, $\chi = 4.6$ eV (graphite work function) - $E_G/2 = 4.3$ eV for the (17,0) nanotube [12]. $\phi_M = 4.5$ eV for a tungusten tip [6,11]. These numbers define the vacuum barrier height. $D(W)$ is calculated with a WKB approximation [9] for each vacuum width d. Equation (2) is then reduced to single integrations using integration by parts, and then a numerical calculation is performed. Image potential [6,9] is not considered, and the semiconductor band bending [6,9] is neglected, but they do not change our qualitative conclusions. S, d, and ξ will be determined to fit the experimental I-V data best.

Comparison with STM tip -nanotube experiment

Figure 5 shows an analysis for the observed type-I I-V pattern with a low tip-to-film distance of 1.85 μm [1]. ξ shifts the entire I-V curve horizontally and the best fit is obtained for $\xi/E_G = 0.65$ (> 0.5). This is consistent with our conclusion of n-nanotube. For very large d such as 0.4 nm, dI/dV asymmetry for opposite polarities is more enhanced than the experiment, and S is unreasonably large ~ 4000 nm^2, compared to the dimension of the 1.36 nm-wide nanotube. This is certainly not the case. S should be less than ~ 10^2 nm^2. d is measured from the natural separation defined by the surface bonding, and there is no lower limit. Therefore, combinations of d ~ 0.1 - 0.2 nm and S ~ 3 - 34 nm^2 in the figure are all in the reasonable range. Since the theoretical curves for these S-d combinations are indistinguishable, we will not narrow it down further.

Compared with the experimental data [1], the calculated voltage interval $\Delta V = E_G/e = 0.54$ V for $I \neq 0$ is wider. However, E_G weakly depends on nanotube diameter, so a large deviation from the above value is unlikely (e.g., E_G is still 0.4 eV for a diameter as wide as 1.8 nm [13]). The semiconductor band bending and the finite temperature (the experiment was carried out at room temperature) are known to reduce ΔV effectively [12], so these could explain the discrepancy. We

do not explicitly include a series resistance R_S representing phenomenologically the bulk nanotube-film resistance and the nanotube film contact resistance to an electrode, etc. R_S is implicitly included in the resistance of the vacuum gap, through d and S. Overall fitting is reasonable, and the results correctly recover large dI/dV with $V > 0$ and small dI/dV with $V < 0$, one of the key experimental findings [1].

Figure 6 shows an analysis for the experimentally observed type-II I-V pattern with a high tip-to-film distance of 1.98 μm [1]. We must explicitly include R_S in this mode. In an equivalent circuit with a Schottky diode and R_S, the diode current I_D, the diode voltage V_D, and the total voltage V are related by $I_D = -I_0[\exp(-\beta V_D) - 1]$ and $V = V_D + I_D R_S$, where β is the inverse temperature. I_0 is a constant related to S and ϕ_n. The diode-only characteristics (V_D, I_D) are plotted in Fig. 3 with $I_0 = 3.53 \times 10^{-18}$ A, resulting in a discrepancy. We thus introduce $R_S = 1.54$ MΩ, and plot the characteristics ($V_D + I_D R_S$, I_D). This recovers the experiment well.

The experimental current level in Fig. 6 is smaller than that in Fig. 5. When the tip-to-film distance is low, the tip-nanotube binding will be weak (physisorption-like) and there will be a vacuum gap, so that S will be large to support the tension on the nanotube from the film. As the tip-to-film distance is higher, the tip-nanotube binding will be stronger and S can become smaller. This is because the tension always tends to reduce S by pulling the nanotube downward. S will be minimized in the touching mode where the binding is strongest (chemisorption-like). In fact, we can recover the above $I_0 \sim 3 \times 10^{-18}$ A by expecting, e.g., $S \sim 0.1$ nm^2 and $\phi_n \sim 0.5$ eV ($< E_G$) with the Richardson constant $A^* \sim 10^1$ Acm^{-2}K^{-2} in $I_0 = SA^*T^2\exp(-\beta\phi_n)$ [6], where T is the temperature. S and ϕ_n in these ranges are possible. For further investigation, mechanical properties of the tip-nanotube contact has to be studied experimentally, and S, ϕ_n, and A^* need to be determined by measuring I as a function of T.

Application to semiconducting nanotube FET with metallic electrodes

The present model can be applied to other cases when a semiconducting nanotube is contacted with a large metal. In recent experiment [2,3,7], the characteristics with rather symmetric dI/dV in both bias polarity separated by ΔV with $I = 0$ (somewhat resembling type-I except the symmetry) have been observed for drain current (I_d) vs. drain voltage (V_d) in nanotube FETs, where the semiconducting nanotube channel (length L) is contacted by metallic source and drain electrodes. As discussed above, the nanotubes are consistently p-type. I_d-V_d characteristics are measured using long ($L \sim 3$ μm, Ref. 3) and short ($L \sim 0.4$ μm, Ref. 7) nanotubes at 4.2 K (carrier freeze-out temperature) with zero gate voltage. In the long L case, the I_d-V_d characteristics are successfully explained by the present model: ΔV is related to E_G, and L-independent. In the short L case, similar characteristics are observed, but they are caused by a fundamentally different mechanism, Coulomb blockade [14]: ΔV is related to the nanotube capacitance for the substrate and the electrodes, and therefore L-dependent. We will not discuss this short L limit further.

In the long L limit, we consider that two independent metal-semiconductor junctions in the vacuum-gap mode are connected back-to-back to form a metal-semiconductor-metal (source-channel-drain) structure, and tunneling occurs at each junction. When $V_d = -E_G/e$ is applied as in Fig. 7(a), the greatest voltage drop in the circuit occurs at the drain junction. An electron tunnels from the drain to the empty conduction band of the p-nanotube: there are practically no thermally excited electrons or even holes in this long p-nanotube at this low temperature. The conduction electron cannot survive until reaching the source, and recombines with a hole immediately. This hole has been generated as a vacant spot of a valence-band electron at the source side, and traveled all the way to the drain side. The generated electron tunnels to the source. When $V_d = E_G/e$

is applied in Fig. 7(b), we will have a band diagram mirror-symmetric to the previous one. Therefore, $\Delta V = 2E_G/e$ (unlike the single junction case of E_G/e) and this is independent of L.

The calculated I_d-V_d characteristics are compared with the experimental characteristics [3] in Fig. 7(c), assuming a (17,0) semiconducting nanotube (the experimental diameter at 1.3 nm [3]) with d = 0.4 nm and S = 406 nm^2 for both source and drain junctions. Since source and drain electrodes are macroscopically wide (~ 0.1 μm), S would be very likely in this range. The calculation reasonably recovers the experimental results [3]. Regardless of possible difference in the source and the drain junctions in reality, the observed curve is reasonably symmetric. This is because whenever conduction band tunneling occurs at one side, valence band tunneling occurs at the other side, and it is this correlation that makes the curve rather symmetric.

It is worth noticing that the I_d-V_d characteristics do not really depend on whether the nanotube is p-type or n-type in the nondegenerate range, or are independent of ξ as is apparent in the band diagram. Mathematically, let $V = r(I)$ be the single-junction characteristics for given ξ, where generally $r(I) \neq -r(-I)$ as we have seen for type-I. The double-junction characteristics are obtained by $V = r(I) - r(-I)$. If we increase ξ by $\Delta\xi$, then $V = r(I) - \Delta\xi$ is the new single-junction characteristics. For a double-junction structure, we form $V = [r(I) - \Delta\xi] - [r(-I) - \Delta\xi] = r(I) - r(-I)$, where $\Delta\xi$ cancels out. Thus, the I_d-V_d characteristics are independent of ξ and have π-rotational symmetry around the origin in the I-V plane as seen in the functional form of $V = r(I) - r(-I)$.

As observed experimentally [3,7], ΔV disappears quickly as the temperature is raised. At 300 K, ΔV completely disappears. We here focus on the role of thermally excited holes in the channel. Because of these holes, the nanotube now conducts current well, without the interruption of ΔV. The corresponding band diagram is shown in Fig. 8 for $|V_d| < E_G/e$. Even with small V_d, an electron can immediately find a hole to recombine, so that it can easily tunnel from the drain to the

nanotube. At the source side of the nanotube, a valence electron leaves a hole and tunnels to the source. As gedanken experiment, if carrier freeze-out temperature is suddenly reached, then the electron cannot find a hole to recombine or an available empty state to tunnel into. Thus, the current is suppressed. We then need to raise $|V_d|$ around E_G/e to have a current onset, so that the electron can find a lot of empty states in the conduction band.

Summary

The two *I-V* patterns observed [1] for the STM tip-nanotube system are explained with a metal-semiconductor contact model. In the vacuum-gap mode, we expect different *dI/dV* at opposite bias polarities reflecting the conduction- and valence-band tunneling, and the existence of ΔV due to the band gap. In the touching mode, the *I-V* characteristics are rectifying, because of the usual Schottky mechanism. We have argued that the Schottky forward transport occurred at the same bias polarity as the valence-band tunneling in the experiment, and concluded that the nanotube was *n*-type. Using the present model, we attribute the *I-V* characteristics observed between the source and the drain in a long-channel nanotube FET [3] at low temperature to two serially connected metal-semiconductor junctions.

Acknowledgement

The author acknowledges M. Meyyappan, T. R. Govindan, R. A. Kiehl (U. of Minesota), and B. A. Biegel for fruitful discussions.

References

[a]CSC, Electronic address: yamada@nas.nasa.gov

[1] P. G. Collins, A. Zettl, H. Bando, A. Thess, and R. E. Smalley, Science **278**, 100 (1997).

[2] S. J. Tans, A. R. M. Verschueren, and C. Dekker, Nature **393**, 49 (1998); R. Martel, T. Schmidt, H. R. Shea, T. Hertel, and Ph. Avouris, Appl. Phys. Lett. **73**, 2447 (1998); T. Yamada, Appl. Phys. Lett. **76**, 628 (2000).

[3] C. Zhou, J. Kong, and H. Dai, Appl. Phys. Lett. **76**, 1597 (2000).

[4] F. Leonard and J. Tersoff, Phys. Rev. Lett. **83**, 5174 (1999)

[5] T. Hertel, R. E. Walkup, and Ph. Avouris, Phys. Rev. B **58**, 13870 (1998).

[6] S. M. Sze, *Physics of Semiconductor Devices*, 2nd ed. (Wiley, New York, 1981).

[7] H. R. Shea, R. Martel, T. Hertel, T. Schmidt, and Ph. Avouris, Microelectronic Engineering **46**, 101 (1999).

[8] D. K. Schroder, *Semiconductor Material and Characterization* (Wiley, New York, 1990).

[9] C. Duke, *Tunneling in Solids*, Suppl. 10 of *Solid State Physics*, edited by F. Seitz and D. Turnbull, (Academic, New York, 1969); J. Bono and R. H. Good, Jr., Surf. Sci. **175**, 415 (1986).

[10] P. Delaney and M. Di Ventra, Appl. Phys. Lett. **75**, 4028 (1999); M. P. Anantram, S. Datta, and Y. Xue, Phys. Rev. B **61**, 14219 (2000).

[11] R. M. Feenstra and J. A. Stroscio, J. Vac. Sci. Technol. B **5**, 923 (1987).

[12] R. Saito, M. Fujita, G. Dresselhouse, and M. S. Dresselhouse, Phys. Rev. B **46**, 1804 (1992), M. S. Dresselhaus, G. Dresselhouse, and P. C. Eklund, *Science of Fullenes and Carbon Nanotubes* (Academic, San Diego, 1996).

[13] J. W. Mintimore and C. T. White, Carbon **33**, 893 (1995). The diameter of 1.3 nm was directly measured with STM in L. C. Venema, J. W. G. Wildöer, J. W. Janssen, S. J. Tans, H. L. J. T. Tuinstra, L. P. Kouwenhoven, C. Dekker, Science **283**, 52 (1999).

[14] D. V. Averin and K. K. Likharev, J. Low Temp. Phys. **62**, 345 (1986); A. Bezryadin, A. R. M. Verschueren, S. J. Tans, and C. Dekker, Phys. Rev. Lett. **80**, 4036 (1998).

Figure Captions

FIG. 1. STM tip-nanotube system with two mechanical contact modes: (a) type-I and (b) type-II *I-V* patterns. (c) shows the vacuum-gap mode and (d) shows the touching mode, where S is the overlap area of the tip and the nanotube and d is their separation distance.

FIG. 2. Electronic transport in STM tip- n-nanotube system. (a) is a type-I *I-V* pattern, and (b) - (d) are band diagrams in the vacuum-gap mode. (e) is a type-II *I-V* pattern, and (f) - (h) are band diagrams in the touching mode.

FIG. 3. Electronic transport in STM tip- p-nanotube system. (a) is a type-I *I-V* pattern, and (b) - (d) are band diagrams in the vacuum-gap mode. (e) is a type-II *I-V* pattern, and (f) - (h) are band diagrams in the touching mode.

FIG. 4. γk_{zS}^2 and W ($= \gamma k_{zM}^2$) are plotted as a function of γk_ρ^2 with E and $\delta = \pm\alpha_i(E - E_i)$ as a parameter, using the parallel momentum-energy conservation relation. Because of the requirement that both functions be positive, the W-integration in Eq. (2) is restricted to $E - \delta = E \pm \alpha_i(E_i - E) \leq W \leq E$.

FIG. 5. Type-I (vacuum-gap) *I-V* characteristics of an STM tip-nanotube system analyzed with the tunneling formula with experimental data for a tip-to-film distance of 1.85 μm from Ref. 1.

FIG. 6. Type-II (touching) *I-V* characteristics of an STM tip-nanotube system analyzed with the Schottky formula with experimental data for a tip-to-film distance of 1.98 μm from Ref. 1.

FIG. 7. Electronic transport of source-nanotube channel-drain structure at freeze-out temperature: (a) and (b) are band diagrams and (c) is the *I-V* characteristics analyzed with two metal-semiconductor junctions connected in series, with experimental data from Ref. 3.

FIG. 8. Band diagram at extrinsic temperature, where current can flow with $|V_d| < E_G/e$ because of many thermally excited holes.

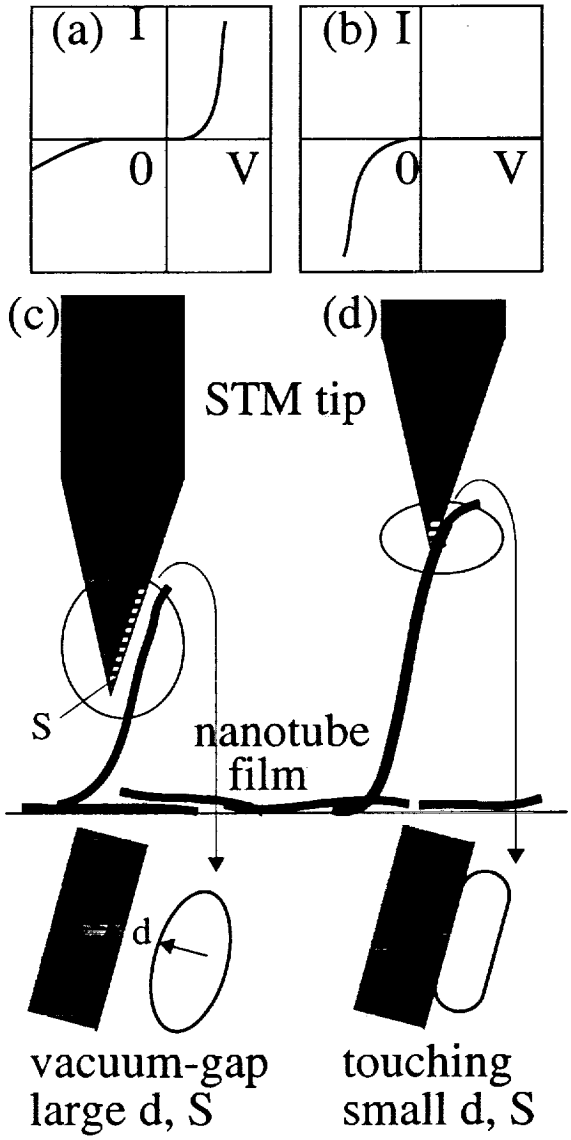

Fig. 1
Toshishige Yamada

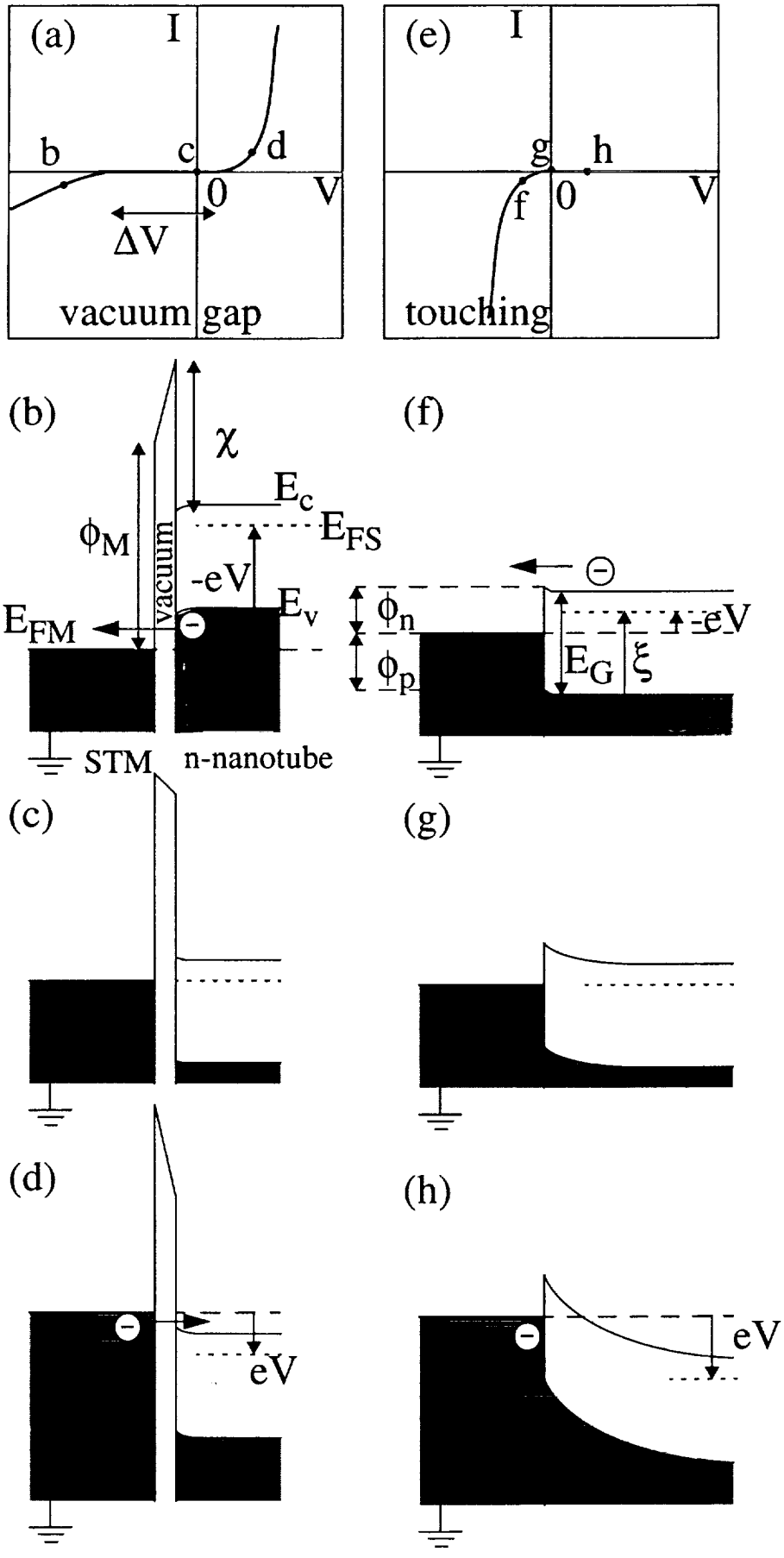

Fig. 2
Toshishige Yamada

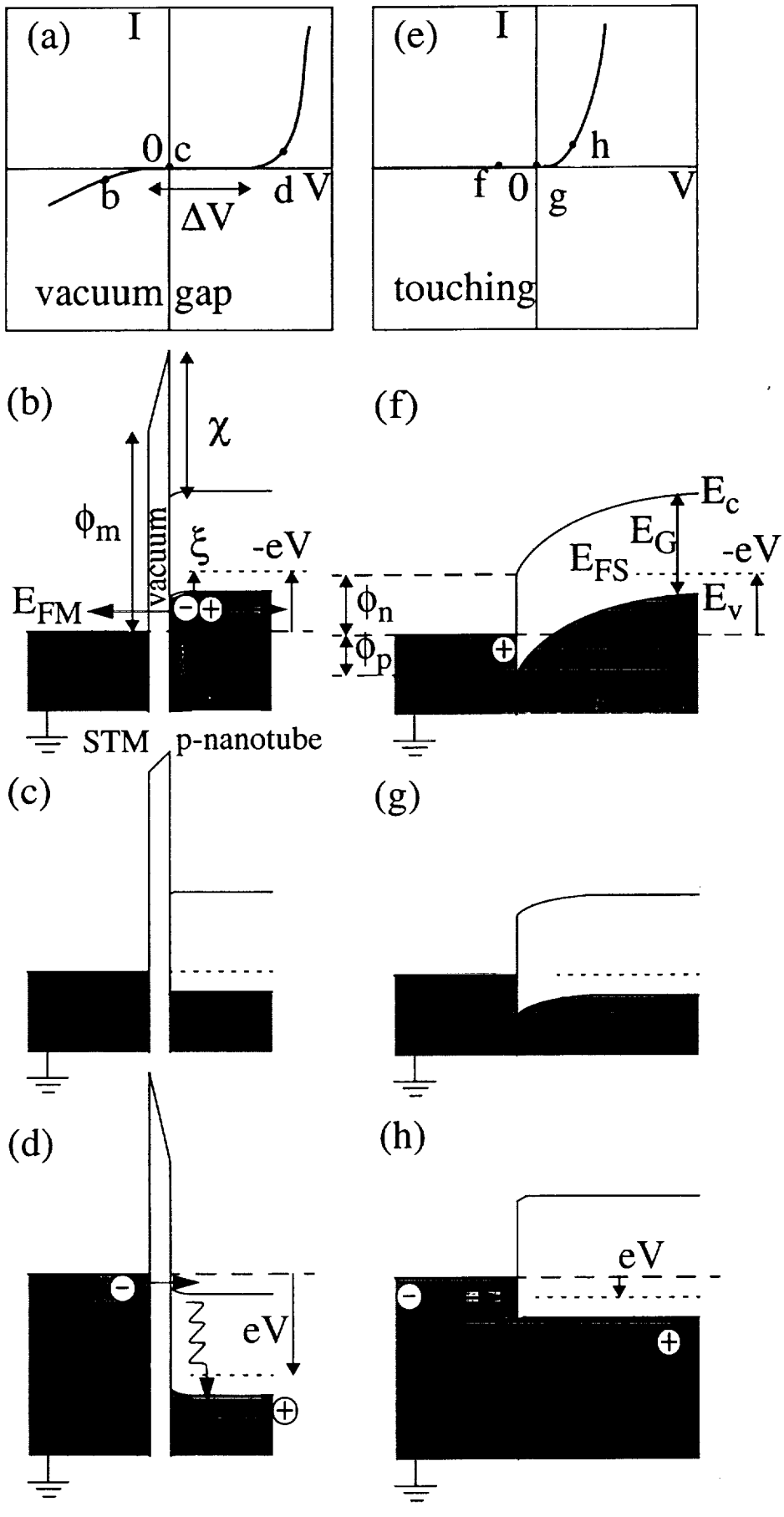

Fig. 3
Toshishige Yamada

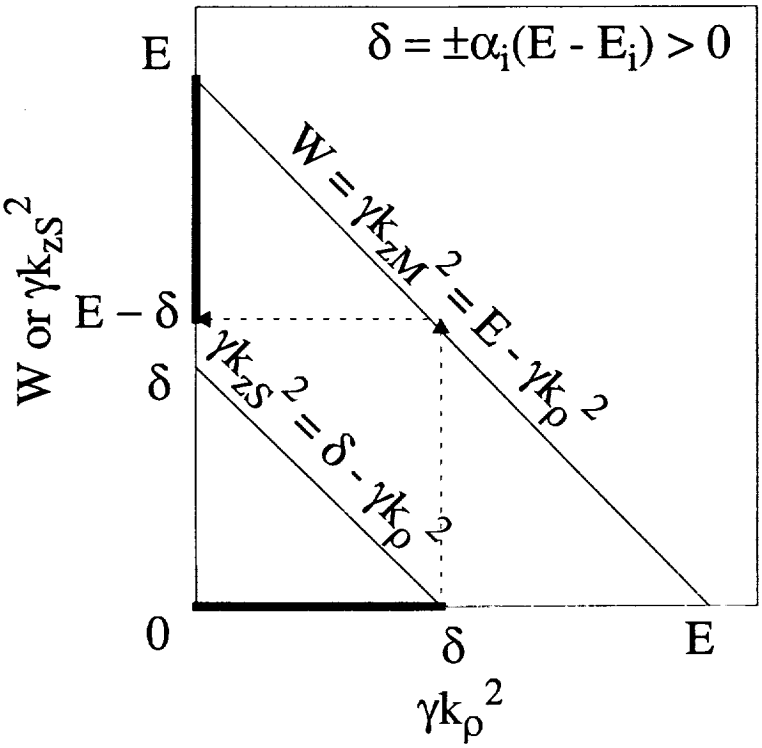

Fig. 4
Toshishige Yamada

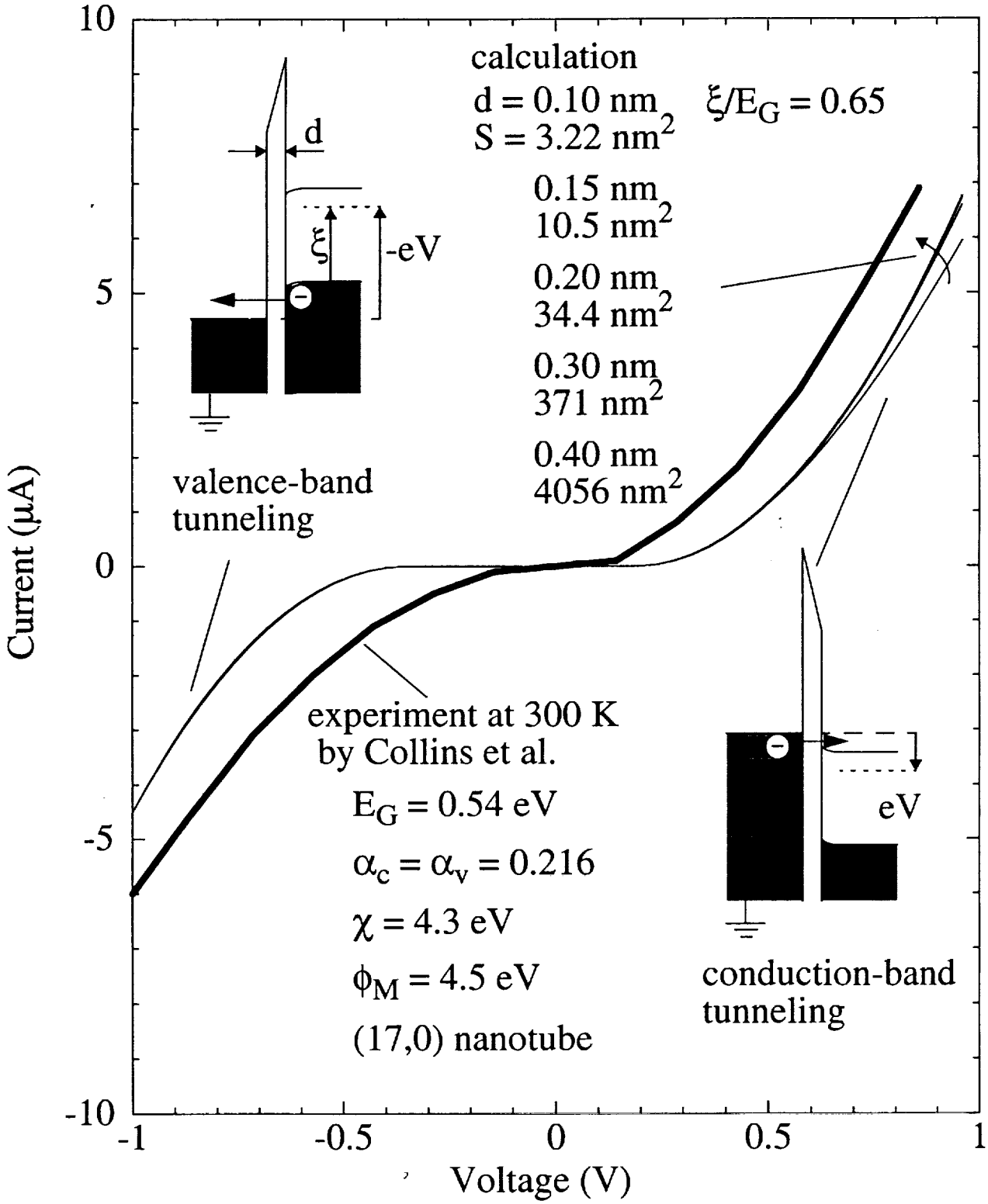

Fig. 5
Toshishige Yamada

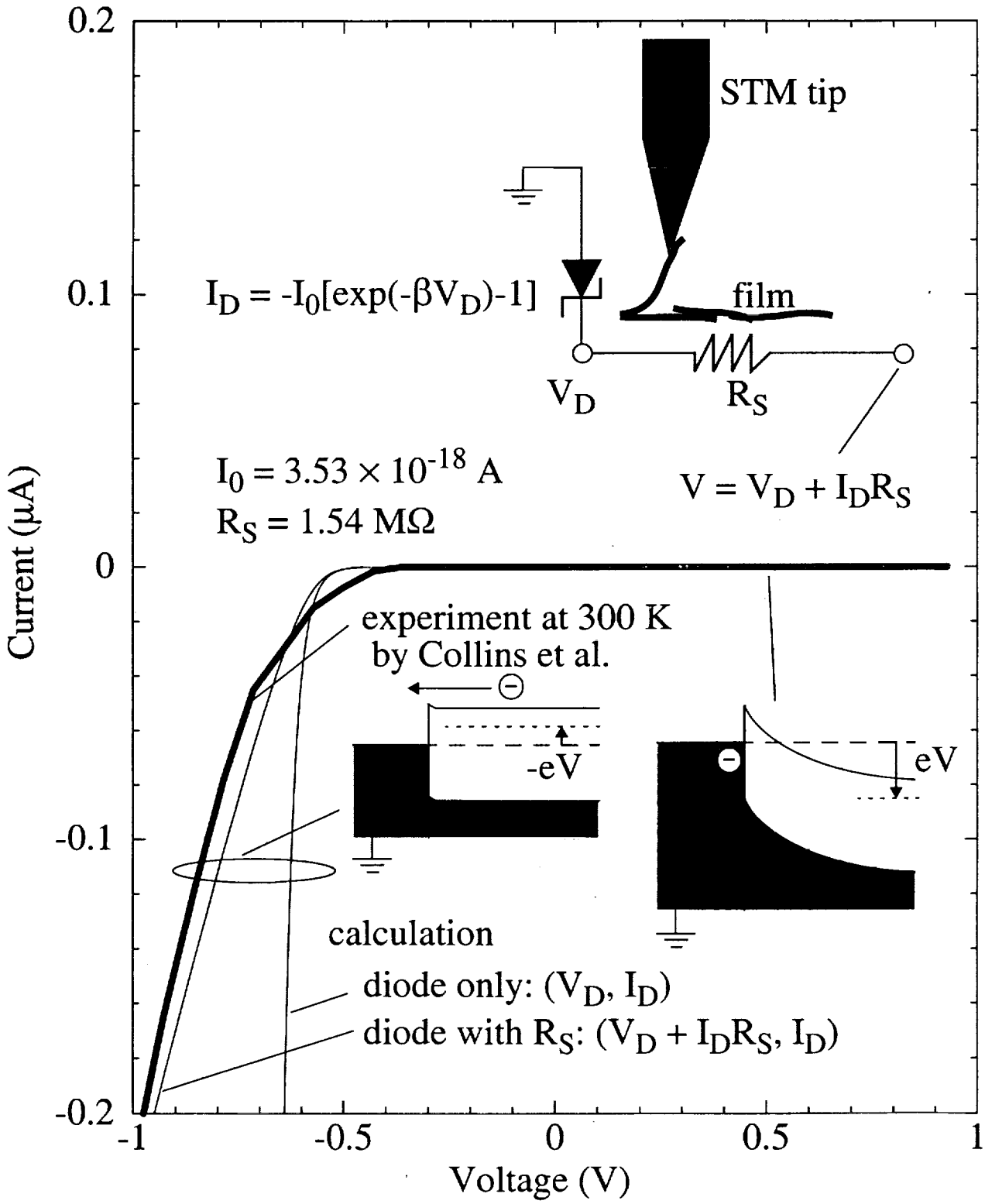

Fig. 6
Toshishige Yamada

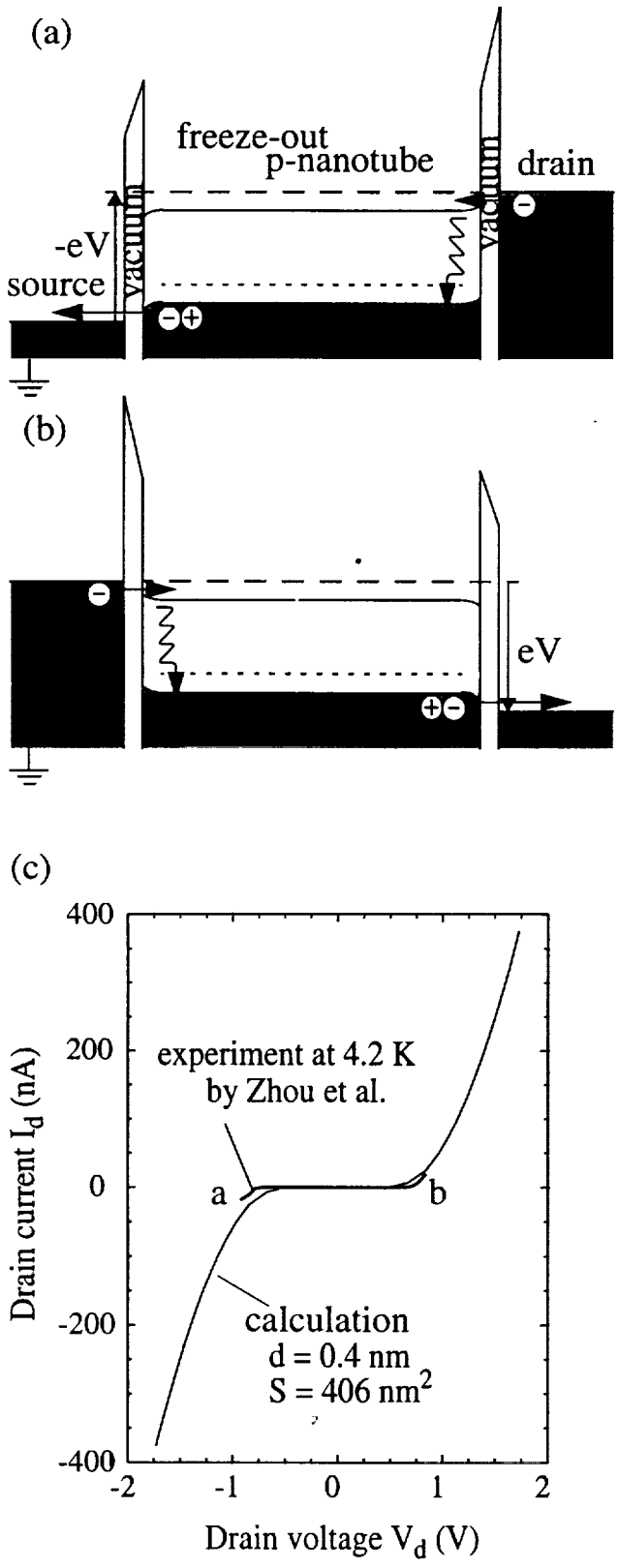

Fig. 7
Toshishige Yamada

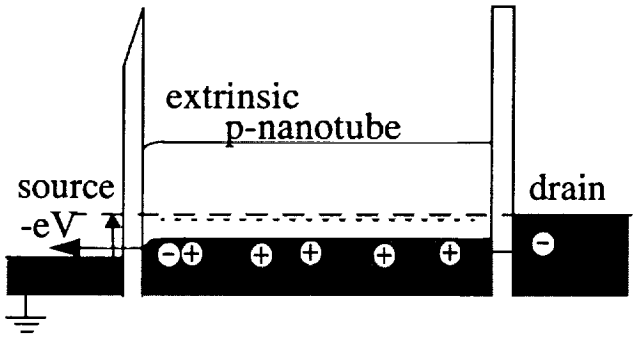

Fig. 8
Toshishige Yamada

(Please use the same scale as the previous Fig. 7)